Marine Pollution Bulletin 165 (2021) 112150

Contents lists available at ScienceDirect

Marine Pollution Bulletin

journal homepage: www.elsevier.com/locate/marpolbul

Plastic debris composition and concentration in the Arctic Ocean, the North Sea and the Baltic Sea

Jari Hänninen [a,*], Markus Weckström [a], Joanna Pawłowska [b], Natalia Szymańska [b], Emilia Uurasjärvi [c], Marek Zajaczkowski [b], Samuel Hartikainen [c,d], Ilppo Vuorinen [a]

[a] Archipelago Research Institute, Biodiversity Unit, FI-20014, University of Turku, Finland
[b] Institute of Oceanology, Polish Academy of Sciences, Powstancow Warszawy Street 55, 81-712 Sopot, Poland
[c] University of Eastern Finland, SIB Labs, P.O. Box 1627, FI-70211 Kuopio, Finland
[d] University of Eastern Finland, Department of Environmental and Biological Sciences, P.O. Box 1627, FI-70211 Kuopio, Finland

ARTICLE INFO

Keywords:
Plastic debris
Marine litter
Arctic Ocean
North Sea
Baltic Sea

ABSTRACT

Neuston samples were collected with a Manta trawl in the rim of the Arctic Ocean, in the Northern Atlantic Ocean and the Baltic Sea at eleven coastal and open-sea locations. All samples contained plastics identified by FTIR microscopy. Altogether, 110 microplastics pieces were classified according to size, shape, and polymer type. The concentrations at the locations were generally low ($\bar{x}$ = 0.06, SD ± 0.04 particles m^{-3}) as compared to previous observations. The highest concentrations were found towards the Arctic Ocean, while those in the Baltic Sea were generally low. The most abundant polymer type was polyethylene. Detected particle types were mainly fragments. The number of films and fibers was very low. The mean particle size was 2.66 mm (SD ± 1.55 mm). Clustering analyses revealed that debris compositions in the sea regions had characteristic differences possibly reflecting the dependences between compositions, drifting distances, sinking rates, and local oceanographic conditions.

1. Introduction

Globally, the extent of plastic pollution (Barnes et al., 2009) has reached also the world's northernmost marine realm. Plastics exist in all investigated environments (see a recent review for European Arctic by Halsband and Herzke, 2019, Tekman et al., 2020) including polar sea-ice and snow (Obbard et al., 2014; Peeken et al., 2018), surface and sub-surface waters (Lusher et al., 2015; Amèlineau et al., 2016; Cózar et al., 2017), biota (Morgana et al., 2018; Peeken et al., 2018), deep-sea sediments (Bergmann and Klages, 2012; Bergmann et al., 2017; Tekman et al., 2017; Kanhai et al., 2019), waste waters, and beaches (Granberg et al., 2019; Von Friesen et al., 2020). The rationale for this study was to find out whether a continuum of surface-dwelling plastic debris particles could be found following the main oceanographic current patterns from the south, in the Baltic Sea, along the Norwegian coast, to the north, up to the Fram Strait. Furthermore, there is a continuum of decreasing anthropogenic environmental impact along the studied route, and this has been the subject of extensive long-term studies by the Institute of Oceanology of the Polish Academy of Science (e.g., Walczowski and Piechura, 2007; Merchel and Walczowski, 2020). Research by the Archipelago Research Institute (ARI) of the University of Turku, Finland has shown the effects of the Baltic Sea brackish water outflow in the North Sea in terms of nutrients, zooplankton, and fish (Hänninen et al., 2015; Hänninen et al., 2021). Therefore, we wanted also to follow the Baltic Sea water, including possible plastic debris, as it mixes with the Norwegian Coastal Slope Current and eventually finds its way up to the north. So far, these adjacent and oceanographically connected marine systems have been studied separately with the least studies concerning the Norwegian coast. We wanted to have a more holistic approach, as the surface currents, which also carry plastic debris, are a unifying factor between these areas.

1.1. The study area

The Arctic Ocean communicates with the world oceans through several passages. The most important for water transport, the Fram Strait (Fahrbach et al., 2001), which lies between Greenland and Svalbard, was, in this study, the most extensively sampled sea region. We

* Corresponding author.
E-mail address: jari.hanninen@utu.fi (J. Hänninen).

https://doi.org/10.1016/j.marpolbul.2021.112150
Received 8 October 2020; Received in revised form 2 February 2021; Accepted 3 February 2021

also placed sampling stations in the West Spitsbergen Current, the Norwegian Coastal Slope Current, and further south along the Norwegian coast and in the Baltic Sea (Fig. 1, Table 1).

Two currents flow through the strait being the West Spitsbergen Current (WSC) that carries waters of Atlantic origin northward on the Svalbard side of the strait with a branch returning towards the Atlantic and the East Greenland Current (EGC) that carries water and sea-ice southward on the Greenland side of the strait (Talley et al., 2011).

Atlantic waters can penetrate the Arctic Ocean also through the Barents Sea. A mix of North Atlantic water with northward flowing Baltic Sea waters (Rudels, 2013) forms the Norwegian Coastal Slope Current (NwCSC). This current has two branches in its northernmost section with one flowing to the Barents Sea and the other forming the WSC and flowing through the Fram Strait (Talley et al., 2011).

The semi-enclosed Baltic Sea is a major brackish water basin (Voipio, 1981). Less saline surface water flows out of the Baltic to the North Sea. The Baltic Sea provides a yearly inflow of about 500 km^3 to the North Sea (OSPAR, 2000). Although the Baltic water input is small compared to the volume of 47,000 km^3 of the North Sea (Hänninen and Vuorinen, 2011), it is very important for the coastal subregions of the North Sea, because the currents keep near the coasts (Radach and Lenhart, 1995). The Baltic outflow leaves the North Sea mainly as a northerly current along the western Norwegian coast (Dooley, 1974; Krause et al., 1995).

2. Materials and methods

2.1. Route description and sampling locations

Samples were collected during the *s/y Oceania*'s AREX2017 (Polish Academy of Sciences) cruise from June 14 to August 30, 2017 from Longyearbyen, Svalbard, Norway to Gdansk, Poland (Supplementary information at: https://www.fiskeridir.no/content/download/24572/338453/version/ 4/file/170122.pdf). Station locations were chosen along separate transects across the Fram Strait, from western Spitzbergen to northern Norway, southwards along the Norwegian coast and finally to the southern Baltic Sea.

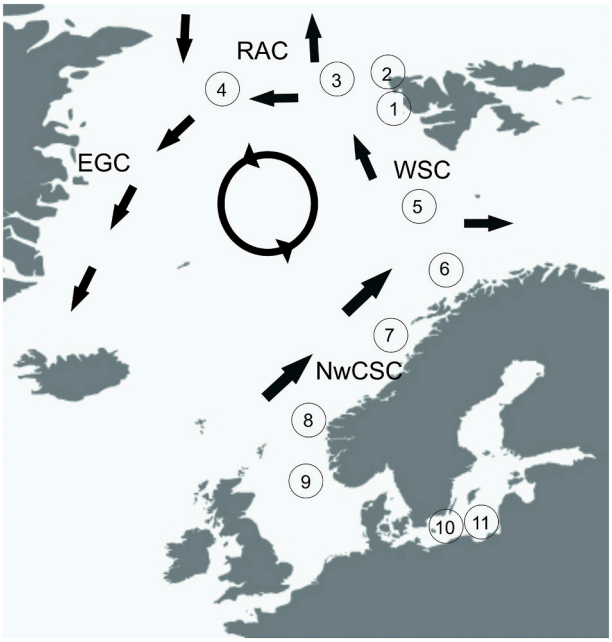

Fig. 1. Main surface currents and the Greenland gyre (based on Håvik et al., 2017), NwCSC=Norwegian Coastal Slope Current, WSC=West Spitsbergen Current, RAC = Return Atlantic Current, EGC = East Greenland Current and plastics sampling locations 1 to 11 during summer 2017. Also, there is an income area for Arctic water NW of RAC. Map: *https://freevectormaps.com/world-maps/WRLD-EPS-01-0008?ref=atr*

Table 1
Indices, names, locations, and descriptions of sampling stations for Manta trawling during the Arex 2017 cruise in 2017. Station locations were chosen on the grounds of surface waters flowing from lower latitudes towards the Arctic at different sections of the current system and adjacent coastal areas.

Index	Geographical name	Latitude	Longitude	Description
1	Soergättet	79°39′ N	10°57′ E	Coastal waters west of Svalbard
2	Magdalenafjord	79°33′ N	11°11′ E	A fjord located in western Svalbard
3	WSC North	79°08′ N	06°59′ E	West Spitsbergen Current, west of Svalbard
4	Hovgaard	78°22′ N	01°20′ E	The center of the Fram Strait
5	WSC South	73°48′ N	18°07′ E	West Spitsbergen Current south of Bjørnøya
6	Norwegian current	70°28′ N	20°01′ E	Eastward branch of Norwegian Current
7	Lofoten mouth	68°07′ N	14°03′ E	The mouth of Lofoten fjord
8	Mid-Norway	63°34′ N	07°03′ E	Norwegian Current west of middle Norway
9	Viken	59°29′ N	05°07′ E	Norwegian coast at northern North Sea
10	Baltic 1	54°55′ N	15°31′ E	Baltic Sea, east of Bornholm
11	Baltic 2	54°55' N	16°34′ E	Open Baltic Sea, close to Polish coast

2.2. From water to a bottle: sampling and sample treatment on-board

Prior to sampling, a CTD probe (Seabird) was used to check that the sampling could be done in locally representative oceanographic conditions. Plastics floating at the uppermost water layer were sampled using a Manta trawl (Oceomic, Marine Bio and Technology S.L., Las Palmas, Spain) with a mesh size of 335 μm and a mouth of 16 cm high and 60 cm wide and equipped with a flowmeter (factor = 0.3 m/propeller turn). The trawl was towed on the side of the ship at a speed of 2.5 knots for approximately 30 min. When dense zooplankton populations were present at the surface layer, the towing time was reduced. The exact towing distance was recorded by a flowmeter, which was placed at the mouth of the trawl.

After the tow, the mesh was carefully washed from the outside with local surface water to ensure that all the collected material had reached the removable cod-end. The cod-end was then detached and placed into a pre-cleaned, covered jar. Sample treatment was conducted in a closed laboratory room wearing a cotton laboratory jacket to avoid fiber contamination. Contents of the cod-end were carefully washed into the jar using filtered Millipore water. Large biological items, such as pieces of kelp, jellyfish, etc. were washed above the jar and then removed. In order to find out possible material that were less than 335 μm, the samples were pre-sieved twice, first with a 200 μm sieve and then with a 50 μm sieve and finally washed into a pre-cleaned glass container.

Fiber contamination during sample treatment was controlled by collecting the fiber fallout into three open Petri dishes placed in the vicinity of the jar. Petri dishes were washed using filtered Millipore water prior to use and sealed with laboratory film after the treatment.

2.3. Sample pre-treatment and identification of plastics

As precautions for contamination, cotton lab coats, nitrile gloves, a fume hood and ultrapure water were used. All glassware was rinsed with ultrapure water. Because collected samples were very rich in organic material, microplastics were isolated for material analysis by digesting and dissolving non-plastic solids with sodium dodecyl sulphate (SDS) and hydrogen peroxide (H_2O_2), which are efficient reagents for

digesting organic materials but do not decompose microplastics (Löder et al., 2017).

First, samples were stored in a SDS solution for several weeks to remove plastic particles from thick natural waxes on the surfaces of seaweeds. Second, samples were sieved through steel sieves of mesh sizes: 4000, 2000, 1000, 750, 300, 150, 106, 63, and 53 μm, which were placed one on top of the other, respectively. Plastics were collected with tweezers from 1000 to 4000 μm sieves. Materials on <1000 μm sieves were rinsed into clean glass containers with MilliQ water for the H_2O_2 digestion. Rinsed sieves were examined visually with a stereo microscope to ensure that all particles were removed. Finally, H_2O_2 was added to the samples until a 15% (vol/vol) concentration was achieved. Samples were first incubated in a 60 °C water bath for 4 h followed by room temperature treatment for 24 h. After peroxide digestion, samples were vacuum filtered with Whatman 113 filter papers, which were stored in Petri dishes.

The microscopy and Fourier-transform infrared spectroscopy (FTIR) analysis methods were adapted from Uurasjärvi et al. (2020), which was done for all potential microplastics in order to determine whether a particle was plastic. Particles remaining on filters were examined using a stereo microscope (Zeiss Stemi 508; 6.3–50× magnification; Axiocam ERc 5 s camera; Carl Zeiss Microscopy GmbH, Jena, Germany). Each particle was first classified based on its color, size, and particle type (shape) following a "Standardized Sorting System" introduced by Crawford and Quinn (2017). Then particles were photographed, and the particle sizes with the largest dimensions were measured. Detected and classified particles were placed with micro-tweezers into clean zinc selenide windows for FTIR measurements. Spectra were measured with an FTIR microscope (PerkinElmer Spectrum Spotlight; PerkinElmer, Waltham, MA, USA) in point mode with a single element MCT detector. Measurements were done in transmission mode using an aperture of 25 × 25 μm, a spectral resolution of 4 cm^{-1}, with 16 scans and a spectral range of 700–4000 cm^{-1}.

Plastic polymers were identified by analysing spectra with Thermo OMNIC 9 software (Thermo Fisher Scientific, Waltham, MA, USA). Each spectrum was compared to spectral reference libraries, including the Hummel Polymer Sample library (Thermo Fisher Scientific) and an in-house measured spectra of textile fibers (Talvitie et al., 2017). If the correlation between sample and reference plastic spectra was >70%, the particle was counted as recognized microplastic. Otherwise, the particle was counted as non-plastic.

2.4. Data exploration

Plastic concentration at each station was calculated by dividing the number of confirmed plastic particles by sampled volume (particles m^{-3}) and by sampled area (particles km^{-2} and m^{-2}). Other key variables calculated for each sampling station were the mean size of detected particles and frequencies of different particle and polymer types. The Supplementary data provides detailed characteristics for each sample on a sample-by-sample basis according to Crawford and Quinn (2017).

Since sampling stations were assumed to represent oceanographically very different conditions, which could not be replicated, straightforward statistical hypothesis testing did not come into question. Instead, the data were explored by applying different clustering analysis approaches, using K-means clustering, to detect possible similarities and dissimilarities between the stations. Numbers of clusters were determined using the "elbow method," i.e., seeking for the number of clusters after which additional clusters do not significantly decrease the total within sum of squares. However, an "elbow point" was not evident for each setup, since the total sum of squares decreased quite linearly towards the maximum number of clusters. In such cases, there was some subjective consideration, so that the number of clusters was kept reasonable while decreasing the total within sum of squares as much as possible. Applied clustering approaches are listed in Table 2. We used BSS (explained or between groups estimate of variance) and WSS (unexplained or within groups estimate) as the measures of the source of the total variation in data expressed as Sum of Squares. The ratio between these two estimates of the population variance is known as the F-test providing the F-ratio and F-probability values.

Table 2
Applied approaches for clustering analysis.

Hypothetical pattern (setup)	Data arrangement	Clustering method
1. Observed polymer type, particle type, and color frequency compositions resemble each other between nearby stations.	Frequency table of detected particle identities at each station, when particle identity is defined as its polymer type, particle type, and color.	K-means clustering, number of clusters 6
2. Small particles represent a proportionally minor share in offshore samples, since their sinking starts sooner.	Frequency table of four different particle size classes at each station defined as the 1st, 2nd, 3rd, and 4th quartile of the whole-size distribution.	K-means clustering, number of clusters 3
3. Total plastic abundance and particle mean size resemble each other between oceanographically similar stations.	Mean size (largest dimension) and observed plastic abundance (particles/m^3) as variables for each station.	K-means clustering, number of clusters 2
4. Of determined variables: polymer type, size, and particle type (shape) are relevant with respect to sinking starting time, and thus the composition of these resembles each other between oceanographically similar stations.	Frequency table of detected particle identities at each station, when particle identity is defined as its polymer type, size class (as above), and particle type.	K-means clustering, number of clusters 5

Results of clustering analysis using setup 2, which analysed possible groupings based on size class frequencies, were further examined to find out if there was a meaningful difference in mean particle sizes between proposed clusters. The proposed cluster, where large size classes dominated, was taken as group 1, and the two other clusters of frequent small- and medium-sized particles were combined to form group 2. The non-parametric Welch's *t*-test was run to compare the means of particle sizes between the two formed groups. The null hypothesis was that the means do not differ, and the alternative hypothesis was that mean particle size is larger in group 1 compared to the other groups.

Results of the other clustering analysis setups were not further analysed because: 1) no relevant information was provided or 2) there were no reasonable variables to analyze. The latter concerns particularly setup 4, in which groupings were based on particle identities defined as its polymer type, size, class, and particle type. The idea was to examine if microplastic compositions, defined through mentioned characteristics, resemble each other between oceanographically similar stations or were random. Within the scope of this study, oceanographical similarity (see also Fig. 1 and Table 1) was determined based on the literature by geographical proximity and a CTD cast prior to the tow.

All the analyses were run using R 3.4.4 software. K-means clustering was conducted using function "kmeans" from the base library, and the "elbow method" for cluster number optimizing was conducted using the function "fviz_nbclust" from the "factoextra" package. The Welch's *t*-test was done using the function "t.test" from the software base library.

3. Results

Altogether, the total volume and area of Manta trawl sieved seawater during the AREX2017 cruise were 2086 m^3 (mean = 189.6 m^3 per station, SD ± 33.9) and 13,035 m^2 (mean = 1185 m^2 per station, SD ± 212), respectively. All samples contained plastic particles (Table 3), the characteristics of the particles are described detailed in the Supplementary data. The mean concentration was 10.08 particles per station (SD ± 7.59), which, in terms of volume, equalled 0.058 particles/m^3

(SD ± 0.043) and in sampled area equalled 9264 particles/km^2 (SD ± 6943) or 0.009 particles/m^2 (SD ± 0.007). The most abundant polymer type was polyethylene (PE, 50.2%), followed by polypropylene (PP) and poly(methyl methacrylate)(PMMA) with 24.1% and 20.2%, respectively. Detected particle types were mainly fragments (80.0%) and films (16.4%). The number of fibers was very low (3.6%). The mean particle size, as the length of the largest dimension, was 2.75 mm (SD ± 1.71 mm). Altogether, 219 particles were analysed with each by FTIR microscopy, by which 110 particles were identified to be plastics. Observations are summarized in Table 3 and in Fig. 2. Contaminating fiber fallout was not detected on Petri dishes. Furthermore, only 3.6% of identified plastic particles were classified as fibers, so there was no concern for overestimating particle concentrations due to fiber contamination during sample treatment.

The results of clustering analysis with four different setups, as described in Table 2, are presented in Table 4. This supports the relevance of setup 4 and possibly also of setups 2 and 3. Setup 4, in which the clustering was based on the frequencies of polymer type, size and particle type, would mean that "each group" represents a distinct sea region and nearby stations along the cruise.

In setup 2, with the smaller particles making a smaller share in offshore samples, the proposed hypothesis might be relevant, since the locations furthest offshore were characterized by larger particles.

Also, in the third group, larger size classes dominate, and samples furthest offshore (4 and 5) were clustered into the third group.

In setup 3, the sample characteristics were total plastic abundance and mean size, and they were expected to resemble each other between oceanographically similar stations. In this case, stations 5, 6, and 9 were again clustered into the same group as was the case with setup 2.

Mean particle size, at stations 4, 5, 6, and 9 as proposed by the clustering in setup 2, was significantly larger than at other stations (Welch's *t*-test: $t = -2.597$, $df = 63.606$, $P = 0.012$, group estimates 4.75 mm and 1.72 mm).

Table 3
Summary of observations for each sample. Plastic concentrations are expressed both in particles/m^3 and particles/km^2 (in parenthesis also as particles/m^2) to allow easy comparison with other studies. Multiple types in particle type and polymer type columns indicate even frequencies. The characteristics of the particles are described in detail in the Supplementary data.

Station	Plastic concent. m^{-3}	Plastic concent. km^{-2} (m^{-2})	Mean size (mm)	Most abundant particle type	Most abundant polymer type
1	0.024	3819 (0.004)	1.19	Fragment	PE
2	0.055	8853 (0.009)	1.74	Fragment	PMMA
3	0.058	9287 (0.010)	2.44	Fragment	PE
4	0.074	11,852 (0.012)	2.05	Fragment	PE
5	0.144	23,117 (0.023)	6.19	Fragment	PE
6	0.019	3032 (0.003)	4.47	Fragment	PS
7	0.012	1973 (0.002)	2.23	Fragment	PE, PP, PMMA
8	0.080	12,773 (0.013)	1.22	Film, Fragment	PP, PMMA
9	0.128	20,534 (0.021)	4.17	Fragment	PE
10	0.022	3554 (0.004)	1.05	Fragment	PE, PP
11	0.019	3112 (0.003)	2.55		
$\bar{x}$	*0.058*	*9264 (0.009)*	*2.66*	Film	PMMA
SD	*± 0.043*	*6943 (0.007)*	*± 1.55*		

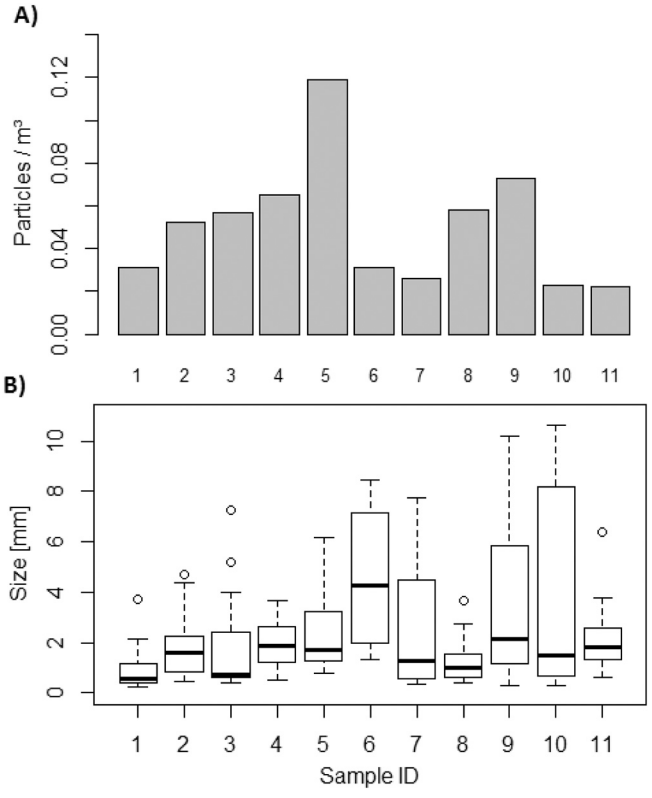

Fig. 4. A) Detected plastic concentrations in particles per cubic meter. **B)** A boxplot for size (largest dimension in millimetres) of detected plastic particles.

4. Discussion

4.1. Concentrations

We found that each studied sample contained plastics, i.e., they were present at each studied section of the current system flowing northward towards the Arctic as well as in coastal waters and fjords.

The highest plastic debris concentration was measured at station 5 close to Bjørnøya. Also, the center area of the Fram Strait (Station 4; Hovgaard) proved to be rich in plastic debris. High concentrations were also found at stations 8 and 9, located in the Norwegian coast at the northern North Sea. This area is probably the most influenced by human populations living in British Isles, Germany, the Netherlands, Scandinavia, and the Baltic Sea countries. The lowest concentrations were detected at stations 6 and 7, along the coastline of northern Norway and, possibly, outside the NwGSC. In general, except at the Baltic Sea locations, variation in concentrations were relatively great. In the Baltic Sea, the concentrations were relatively low, if one expects higher plastic concentrations in the Baltic, whose coasts are heavily populated.

The Baltic Sea comparisons must be taken with caution. Ory et al. (2020) found a low, 0.04 particles m^{-3}, microplastic concentration in the Kiel Fjord with highest concentrations sampled after snow or rainfall. Schönlau et al. (2020) reported a median microplastic particle concentration in the Swedish waters of the Baltic Sea of 0.04 particles m^{-3} from Manta trawling and 0.10 particles m^{-3} in pump samples with a mesh size of 0.3 mm. The highest concentrations were recorded on the west coast of Sweden. Thus, low concentrations in the Baltic might be, for instance, due to lower sea water density and hence more rapid sinking from the surface. That would, in turn, suggest a future sediment study.

Table 4
Results of clustering analysis using four different setups (hypothetical patterns), which are described in Table 2. BSS refers to between sum of squares and WSS refers to within sum of squares. Groupings are expressed using station indices.

Setup	Data arrangement	BSS / WSS	Proposed groupings	Conclusion
1. Observed polymer type, particle type, and color frequency compositions resemble each other between nearby stations.	Frequency table of detected particle identities at each station, when particle identity is defined as its polymer type, particle type, and color.	87.2%	*1,3,6,7,10 2,11 4 5 8 9*	Proposed groupings are oceanographically completely random, and thus no relevant information was obtained.
2. Small particles represent a proportionally minor share in offshore samples, since their settling onset time is shorter.	Frequency table of four different particle size classes at each station, defined as the 1st, 2nd, 3rd, and 4th quartile of the whole-size distribution.	66.9%	*1,11 2,3,7,8,10 4,5,6,9*	In the third group, larger size classes dominate, and samples furthest offshore (4 and 5) were clustered into the third group. Thus, the proposed hypothesis might be relevant.
3. Plastic compositions characterized by total plastic abundance and mean size resemble each other between oceanographically similar stations.	Mean size (largest dimension) and observed plastic abundance (particles/m^3) as variables for each station.	83.9%	*1,2,3,4,7,8,10,11 5,6,9*	Stations 5, 6 and 9 were again clustered into the same group, as with setup 2.
4. Of the determined variables, the polymer type, size, and particle type (shape) are relevant with respect to sinking start time, and thus composition of these resemble each other between oceanographically similar stations.	Frequency table of detected particle identities at each station, when particle identity is defined as its polymer type, size, class (as above), and particle type.	77.8%	*1,2,3,4,5 6,7,8,9 10,11*	Groupings are oceanographically relevant; each group represents distinct sea region and nearby stations along the cruise are clustered into same groups.

Concentrations were generally comparable in other sea regions with global overviews provided, for instance, by Lusher (2015). Direct areal comparisons are not justified due to high variability in methodology. However, based on a table in PAME (2019): Lusher et al. (2015) reported a particle density of 0–1.31 m^{-3} (SD 0.34 ± 0.31) with a Manta net, and 0–11.5 m^{-3} with a seawater pump on-board from a transect from northern Norway up to southwest Svalbard in 2014; Cózar et al. (2017) reported, in year 2013, in the Barents Sea and the Greenland Sea, a density of 0.063 items m^{-2} sampled with a Manta net; Amèlineau et al. (2016) reported in the Greenland Sea, 205 microplastics with a density of 0.15–2.64 m^{-3} (WP-2 net, mesh 500 μm) and in 2014, a density of 0.81–4.52 m^{-3};

Morgana et al. (2018) reported, in the Greenland Sea, a density of 1–3 items m^{-3}; and Kanhai et al. (2018) reported 0–7.5 particles m^{-3} in the Arctic Central Basin sampled with an on-board water pump.

Furthermore, in 2016, Kanhai et al. (2020) reported microplastic concentrations ranging between 0 and 18 fragments m^{-3} in seawater beneath ice flows in the Central Arctic Basin, and Tekman et al. (2020) reported from 113 to 1237 particles m^{-3} in surface water in the Fram Strait. Our mean concentration of 0.05 particles m^{-3} (SD ± 0.03) is comparable.

4.2. The shape and material of polymers

Kanhai et al. (2018) stated that fibrous microplastics and the synthetic polymer polyester (PES) predominate in the Arctic Central Basin. A review by Halsband and Herzke (2019) demonstrates the variety of plastic polymer types found in the European Arctic. In our results, the majority (50.2%) was made of PE, as film-shaped fragments are dominated by PE (Barnes et al., 2009), while in most of the studies, i.e., four cases out of the total of five listed by Halsband and Herzke (2019), the predominating polymer has been PES. PP was, in our samples, the second in predominance (24.1%), which is about the same level that Morgana et al. (2018) reported.

An important feature of the resulting data was that fibers were practically absent, which is in contrast to previous works in the studied sea regions, especially surface sampling between Svalbard and Bjørnøya by Lusher et al. (2015). In their report, 95% of found plastics were fibers. It is possible that the sampling method did not allow for fiber collection, for instance, towing speed or rinsing pressure forced them through the mesh. This reasoning is probable. As Ryan et al. (2020) describe for missing fibers, 300–500 μm mesh nets are too coarse to sample most textile fibers. Also, the visual selection of particles to FTIR microscopy is prone to subjective bias, especially for particle sizes of less than 300 μm (Koelmans et al., 2019). Ryan (2010), who studied plastic debris compositions from shore to offshore in coastal South Africa, concluded that rapid settling occurs if the surface area to volume ratio is high, which supports the idea of low concentrations in offshore samples. Some researchers exclude fibers from their results even if detected, since it is very difficult to be sure that they are truly collected from sampled seawater (Cózar et al., 2017).

Four of the eleven stations expressed greater than average particle sizes between sampling locations. Those were mainly found at areas where debris concentrations were highest. Two of these stations were located in areas with divergent loading from many sources with a pollution load from several countries on the northern North Sea near the Norwegian coast. On the other hand, large particles were found in remote offshore areas at the center of the Fram Strait and off Bjørnøya, which, according to the clustering analysis, might be an indication of a long particle settling time for larger particles. Elsewhere, there was no clear pattern in mean particle size between sampled stations. Instead, those expressed more even variation than between stations.

4.3. Clustering analysis

Probably the most interesting clustering analysis conducted was the one with setup 4 (Table 4), in which the clustering was based on frequencies of particle identities defined through the polymer type, size and particle type. This setup would result in four oceanographically relevant groups being the transformed Atlantic water between Svalbard and Greenland (stations 1–4), the sea region close to Bjørnøya (station 5), the Atlantic waters at the Norwegian coast (stations 6–8), the North Sea waters (station 9) and the Baltic Sea waters (stations 10 and 11). The BSS/WSS ratio was not particularly high (83.9%), and naturally, it is questionable to define groups composed of only one station. To avoid oversimplifying and overinterpretation, the analysis was not taken further. Oceanographic similarity between the proposed groups is here best considered qualitatively, since each straightforward parameter, such as the distance from shore, would oversimplify and distort the issue. Proposed groups refer to samples taken from distinct sea regions, and thus the grouping is oceanographically relevant. Hence, we suggest that areal plastic compositions might have characteristic patterns in oceanographically different sea regions. The main characterizing parameters seemed to be those affecting particles' sinking properties such as polymer type, an indicator of density and size, and particle type, as an indicator of particle weight and shape. Since the groupings were based on properties affecting the sinking velocity, the finding implies that there might be a difference in the ratio between locally discharged

particles versus long-range drifters.

Another interesting outcome was achieved using the setup 2 (Tables 2 and 4), which analysed size class frequencies at sampling stations. Large-size classes dominated at stations 4, 5, 6 and 9, which formed one group in the clustering analysis. Furthermore, mean particle size in the proposed group was proven to be significantly larger than at the rest of the stations (see Welch's *t*-test). The setup was designed hypothesising that offshore samples contain larger plastics, and this assumption was supported. Stations 4 and 5 were furthest offshore, and it is possible that surface waters in station 6 have been flowing quite a long time without a significant influence from coastal settlements. However, results from station 9, belonging to this group, are less logical. Sampled surface water there could have been drifting further offshore for a long time. The result supports discussions above concerning the analysis with setup 4 as particle size, which affects the starting time of the sinking (Ryan, 2010), was larger in the offshore samples.

Clustering analysis using setup 1 was similar to setup 4 with the distinction that color was an additional parameter defining particle identity. The hypothesis was that in the same regions, particles have similar origins, and thus also particle colors are more similar. This resulted in oceanographically random groupings, which could be taken as indirect qualitative evidence for conclusions above regarding setup 4, as properties affecting settling onset time determine the composition, since color, which does not affect it, breaks the relevant grouping. Clustering analysis using setup 3, exploring particle sizes and total abundances between the stations, resulted in a somewhat similar grouping as the setup 2. However, no additional information was provided. Total abundances varied significantly between stations in the same group. Particle size determined groupings, and it was already analysed in detail.

In conclusion, clustering analyses provided interesting insights into the data and implied that plastic compositions in different sea regions might have characteristic differences, which are based on properties that affect particles sinking. It seems that plastic compositions in offshore samples, such as those collected from high northern latitudes in Bjørnøya (station 5) or closest to Greenland (station 4), are indeed dominated by long-range drifters.

4.4. What can be said about the long-range drifting?

The origin of the detected plastic particles could be estimated, if the times spent drifting in seawater could be determined and combined with ocean-current models. At present, however, analytical methods for estimating the plastic drifting times do not exist, and thus only qualitative estimates can be made. In the sample collected from station 5, for instance, many particles were remarkably deteriorated when inspected visually, and since there are no possible local land-based pollution sources, it seems likely that collected plastics were long-range drifters. Also, in the clustering analysis, which clustered station 5 into the group of more frequent large-sized plastics, and a subsequent Welch's *t*-test, supported the idea. However, for now, it is impossible to know for how long long-range drifters have been drifting in the ocean or if they originated from the nearest shore or possibly from the other side of the ocean.

Since all samples contained plastics, and because the sampled waters generally flow northwards, it is logical to infer that if the plastics do not somehow disappear from the surface layer, there should be a continuous in flow of drifting plastic debris into the Arctic. Size distributions implied that long-range drifters were present in the samples. If in-flow rates exceed out-flow rates, there should also be an accumulation happening somewhere, whether in surface waters, the water column, the sea ice, in deep-sea sediments or in the biota.

Supplementary data to this article can be found online at https://doi.org/10.1016/j.marpolbul.2021.112150.

CRediT authorship contribution statement

Jari Hänninen: Project administration, Conceptualization, Funding acquisition, Resources, Writing - review & editing, Supervision. **Markus Weckström:** Methodology, Investigation (r/v *Oceania*), Formal lab analysis, Validation, Writing - review & editing. **Joanna Pawlowska:** Investigation (r/v *Oceania*), Writing - review & editing. **Natalia Szymańska:** Investigation (r/v *Oceania*), Writing - review & editing. **Emilia Uurasjärvi:** Formal lab analysis, Writing - review & editing, Validation. **Marek Zajaczkowski:** Resources, Writing - review & editing, Project administration (r/v *Oceania*). **Samuel Hartikainen:** Lab Methodology, Resources, Supervision. **Ilppo Vuorinen:** Conceptualization, Writing - original draft, Visualization.

Declaration of competing interest

The authors declare that they have no known competing financial interests or personal relationships that could have appeared to influence the work reported in this paper.

Acknowledgements

The project was kindly funded and supported by the Turku University Foundation [grant number 5-707] and by the Rotary Club Nauvo. This study utilized research infrastructure facilities provided by FINMARI (Finnish Marine Research Infrastructure consortium). We thank anonymous referees for comments on an early and later versions of this paper. Robert M. Badeau, M.Sc., Ph.D., of Aura Professional English Consulting, Ltd. (www.auraenglish.com), provided the English language checking service for this manuscript.

References

Amèlineau, F., Bonnet, D., Heitz, O., Mortreux, V., Harding, A.M.A., Karnovsky, N., Walkuszm, W., Fortm, J., Grèmillet, D., 2016. Microplastic pollution in the Greenland Sea: background levels and selective contamination of planktivorous diving seabirds. Environ. Pollut. 219, 1131–1139. https://doi.org/10.1016/j.envpol.2016.09.017.

Barnes, D.K.A., Galgani, F., Thompson, R.C., Barlaz, M., 2009. Accumulation and fragmentation of plastic debris in global environments. Philos. T. R. Soc. B. 364, 1985–1998. https://doi.org/10.1098/rstb.2008.0205.

Bergmann, M., Klages, M., 2012. Increase of litter at the Arctic deep-sea observatory HAUSGARTEN. Mar. Pollut. Bull. 64, 2734–2741. https://doi.org/10.1016/j.marpolbul.2012.09.018.

Bergmann, M., Wirzberger, V., Krumpen, T., Lorenz, C., Primpke, S., Tekman, M.B., Gerdts, G., 2017. High quantities of microplastic in Arctic deep-sea sediments from the HAUSGARTEN observatory. Environ. Sci. Technol. 51, 11000–11010. https://doi.org/10.1021/acs.est.7b03331.

Cózar, A., Marti, E., Duarte, C.M., Garcìa-de-Lomas, J., van Sebille, E., Ballatore, T.J., Eguíluz, V.M., González-Gordillo, J.I., Pedrotti, M.L., Echevarría, F., Troublè, R., Irigoien, X., et al., 2017. The Arctic Ocean as a dead end for floating plastics in the North Atlantic branch of the thermohaline circulation. Sci. Adv. 3 (4), e1600582 https://doi.org/10.1126/sciadv.1600582.

Crawford, C.B., Quinn, B., 2017. Microplastic separation techniques. In: Microplastic Pollutants. Elsevier, Oxford, UK, ISBN 9780128094068, pp. 203–218.

Dooley, H.D. (1974). Hypothesis concerning the circulation of the northern North Sea. *J. Cons. Int. Explor. Mer* 36: 54–61. doi: /10.1093/icesjms/36.1.54.

Fahrbach, E., Meincke, J., Østerhus, S., Rohardt, G., Schauer, U., Tverberg, V., Verduin, J., 2001. Direct measurements of volume transports through Fram Strait. Polar Res. 20 (2), 217–224. https://doi.org/10.3402/polar.v20i2.6520.

Granberg, M., Von Friesen, L. W., Bach, L., Collard, F., Gabrielsen, G.W. & Strand, J. (2019). Anthropogenic microlitter in wastewater and marine samples from Ny-Ålesund, Barentsburg and Signehamna, Svalbard. Rep n:o C373. 28 pp. ISBN 978-91-7883-020-6.

Halsband, C., Herzke, D., 2019. Plastic litter in the European Arctic: what do we know? Emer. Contam. 5, 308–318. https://doi.org/10.1016/j.emcon.2019.11.001.

Hänninen, J., Vuorinen, I., 2011. Time-varying parameter analysis of the Baltic Sea freshwater runoffs. Environ. Model. Assess. 16, 53–60. https://doi.org/10.1007/s10666-010-9231-5.

Hänninen, J., Vuorinen, I., Rajasilta, M., Reid, P.C., 2015. Response of the Baltic and north seas to river runoff from the Baltic watershed—physical and biological changes. Prog. Oceanogr. 138, 91–104. https://doi.org/10.1016/j.pocean.2015.09.001.

Hänninen, J., Mäkinen, K., Rajasilta, M., Vuorinen, I., 2021. The Baltic Sea and the adjacent North Sea silicate concentrations. Estuar. Coast. Shelf Sci. 249, 107110. https://doi.org/10.1016/j.ecss.2020.107110.

Håvik, L., Pickart, R.S., Våge, K., Torres, D., Thurnherr, A.M., Beszczynska-Möller, A., Walczowski, W., von Appen, W.-J., 2017. Evolution of the East Greenland current from Fram Strait to Denmark Strait: synoptic measurements from summer 2012. J. Geophys. Res. Oceans. 122 https://doi.org/10.1002/2016JC012228.

Kanhai, L.D., Gårdfeldt, K., Lyashevska, O., Hassellöv, M., Thompson, R.C., O'Connor, I., 2018. Microplastics in sub-surface waters of the Arctic Central Basin. Mar. Pollut. Bull. 130, 8–18. https://doi.org/10.1016/j.marpolbul.2018.03.011.

Kanhai, L.D., Johansson, K., Frias, C., Gardfeldt, J.P.G.L., Thompson, R.C., O'Connor, I., 2019. Deep sea sediments of the Arctic Central Basin: a potential sink for microplastics. Deep-Sea Res. Pt I. 145, 137–142. https://doi.org/10.1016/j.dsr.2019.03.003.

Kanhai, L.D., Katarina, K.G., Krumpen, T. & Thompson, R.C. (2020). Microplastics in sea ice and seawater beneath ice floes from the Arctic Ocean. *Scientific Reports* 10:5004. doi.org/10.1038/s41598-020-61948-6.

Koelmans, A., Mohamed-Nor, N.H., Hermsen, E., Kooi, M., Mintenig, S.M., De France, J., 2019. Microplastics in freshwaters and drinking water: critical review and assessment of data quality. Water Res. 155, 410–422. https://doi.org/10.1016/j.watres.2019.02.054.

Krause, M., Dippner, J.W., Beil, J., 1995. A review of hydrographic controls on the distribution of zooplankton biomass and species in the North Sea with particular reference to a survey conducted in January–march 1987. Prog. Oceanogr. 35, 81–152. https://doi.org/10.1016/0079-6611(95)00006-3.

Löder, M.G.J., Orcid, H.K., Orcid, I., Ladehoff, M., Löschel, L.A., Lorenz, C., Mintenig, S. Pieh, S., Primpke, S., Schrank, I., Laforsch, C. & Gerdts, G. (2017). Enzymatic purification of microplastics in environmental samples. *Environ. Sci. Technol.* 51: 14283–14292. doi: https://doi.org/10.1021/acs.est.7b03055.

Lusher, A., 2015. Microplastics in the Marine Environment: Distribution, Interactions and Effects. *Mar. Anthrop. Litt.* Springer, Switzerland, In, pp. 245–307. https://doi.org/10.1007/978-3-319-16510-3.

Lusher, A., Tirelli, V., O'Connor, I., Officer, R., 2015. Microplastics in Arctic polar waters: the first reported values of particles in surface and subsurface samples. Sci. Rep. 5, 14947. https://doi.org/10.1038/srep14947.

Merchel, M. & Walczowski, W. (2020). Increases in the temperature and salinity of deep and intermediate waters in the West Spitsbergen current region in 1997-2016. Oceanologia 62, 501–51. doi: 10.1016/ j.oceano.2020.08.001.

Morgana, S., Ghigliotti, L., Estévez-Calvar, N., Stifanese, R., Wieckzorek, A., Doyle, T., Christiansen, J.S., Faimali, M. & Garaventa, F. (2018). Microplastics in the Arctic: a case study with sub-surface water and fish samples off Northeast Greenland. *Environ. Pollut.* 242 Part B: 1078-1086. doi: 10.1016/ j.envpol.2018.08.001.

Obbard, R.W., Sadri, S., Wong, Y.Q., Khitun, A.A., Baker, I., Thompson, R.C., 2014. Global warming releases microplastic legacy frozen in Arctic Sea ice. Earths Future 2, 315–320. https://doi.org/10.1002/2014EF000240.

Ory, N. C., Lehmann, A., Javidpour, J., Stöhr, R.,Walls G.L. & Clemmesen, C. (2020). Factors influencing the spatial and temporal distribution of microplastics at the sea surface–a year-long monitoring case study from the urban Kiel Fjord, southwest Baltic Sea. Sci. Total Environ. 736: 139493. doi: 10.1016/ j.scitotenv.2020.139493.

OSPAR (2000). Oslo & Paris Commission Quality Status Report 2000 - region II greater North Sea. OSPAR Commission, London. 136 + xiii pp. ISBN: 0 946956 48 0.

PAME (2019). Desktop Study on Marine Litter including Microplastics in the Arctic. http://hdl.handle.net/11374/2389.

Peeken, I., Bergmann, M., Gerdts, G. Katlein, C., Krumpen, T. Primpke, S. & Tekman, M. B. (2018). Microplastics in the Marine Realms of the Arctic with Special Emphasis on Sea Ice (Arctic Report Card 2018, ww.arctic.noaa.gov/Report-Card.: 89–99.

Radach, G., Lenhart, H.J., 1995. Nutrient dynamics in the North Sea: fluxes and budgets in the water column derived from ERSEM. Neth. J. Sea Res. 33, 301–335. https://doi.org/10.1016/0077-7579(95)90051-9.

Rudels, B., 2013. Arctic Ocean circulation, processes and water masses: a description of observations and ideas with focus on the period prior to the international polar year 2007-2009. Prog. Oceanogr. 132, 22–67. https://doi.org/10.1016/j.pocean.2013.11.006.

Ryan, P.G., 2010. Does size and buoyancy affect the long-distance transport of floating debris? Environ. Res. Lett. 10, 084019 https://doi.org/10.1088/1748-9326/10/8/084019.

Ryan, P.G., Suaria, G., Perold, V., Pierucci, A., Bornman, T.G., Aliani, S., 2020. Sampling microfibres at the sea surface: the effects of mesh size, sample volume and water depth. Environ. Pollut. 258, 113413. https://doi.org/10.1016/j.envpol.2019.113413.

Schönlau, C., Karlsson, T.T., Rotander, A., Nilsson, H., Engwall, M., Van Bavel, B., Kärrman, A., 2020. Microplastics in sea-surface waters surrounding Sweden sampled by manta trawl and in-situ pump. Mar. Pollut. Bull. 153, 111019. https://doi.org/10.1016/j.marpolbul.2020.111019.

Talley, L., Pickard, G., Emery, W., Swift, J., 2011. Arctic Ocean and Nordic seas. In: Descriptive Physical Oceanography. Elsevier, Oxford, UK, ISBN 9780750645522, pp. 401–436.

Talvitie, J., Mikola, A., Setälä, O., Heinonen, M., Koistinen, A., 2017. How well is microlitter purified from wastewater? – a detailed study on the stepwise removal of microlitter in a tertiary level wastewater treatment plant. Water Res. 109, 164–172. https://doi.org/10.1016/j.watres.2016.11.046.

Tekman, M., Krumpen, T., Bergmann, M., 2017. Marine litter on deep Arctic seafloor continues to increase and spreads to the north at the HAUSGARTEN observatory. Deep-Sea Res. 120, 88–99. https://doi.org/10.1016/j.dsr.2016.12.011.

Tekman, M.B., Wekerle, C., Lorenz, C., Primpke, S., Hasemann, C., Gerdts, G., Bergmann, M., 2020. Tying up loose ends of microplastic pollution in the Arctic: distribution from the sea surface through the water column to Deep-Sea sediments at the HAUSGARTEN observatory. Environ. Sci. Technol. 54, 4079–4090. https://doi.org/10.1021/acs.est.9b06981.

Uurasjärvi, E., Hartikainen, S., Setälä, O., Lehtiniemi, M., Koistinen, A., 2020. Microplastic concentrations, size distribution, and polymer types in the surface waters of a northern European lake. Water Environ. Res. 92, 149–156. https://doi.org/10.1002/wer.1229.

Voipio, A. (1981). The Baltic Sea. *Elsevier Oceanography Series* 30. 417 pp. Elsevier, Amsterdam. eBook ISBN: 9780080870687.

Von Friesen, L.W., Granberg, M.E., Pavlova, O., Magnusson, K., Hassellov, M., Gabrielsen, G.W., 2020. Summer sea ice melt and wastewater are important local sources of microlitter to Svalbard waters. Environ. Int. 139, 105511. https://doi.org/10.1016/j.envint.2020.105511.

Walczowski, W., Piechura, J., 2007. Pathways of the Greenland Sea warming. Geophys. Res. Lett. 33, 1–5. https://doi.org/10.1029/2007GL029974.